Spectral and discontinuous Galerkin methods applied to neutron star magnetospheres

Jérôme Pétri

ISSI Berne - December, 2019

Our goal

Compute realistic neutron star magnetospheres

We need efficient algorithms to catch all the spatial and time scales involved in neutron star electrodynamics.
Many problems to deal with realistic computations

- relevant length scale of magnetosphere is $r_L = c/\Omega$.
- but for slow pulsars, $R/r_L \ll 1$.
- resolution too high in 3D, computational memory and time consuming

$\Rightarrow$ unfeasible.

- time scale of gyroperiod $\ll$ pulsar period.

$\Rightarrow$ impossible to guess relevant time scales appropriate to pulsar magnetospheres.

- downscaling forbidden because the problem is highly non linear.
- everybody has to make some compromises in order to perform (unrealistic) simulations.

Unrealistic magnetospheres: compromises

Basically, two different approaches

- keep a (multi-)fluid description able to model large scales faithfully.

$\Rightarrow$ kills non thermal particle acceleration

$\Rightarrow$ possibility of test particles

- use a kinetic description with Vlasov of PIC methods.

$\Rightarrow$ unable to put realistic pulsar parameters.

$\Rightarrow$ downscaling at the expense of missing the right physics.

Force-free magnetospheres

- Almost FFE simulation
  - ✦ force-free electromagnetic field.
  - ✦ time evolution of Maxwell equations.
  - ✦ current along **B** not included.
  - ✦ formation of a current sheet.
- Limitations
  - ✦ cartesian geometry even for the star surface.
  - ✦ ratio $R/r_{\rm L} = 0.2$ too large $\Rightarrow P = 1$ ms.
- Remedies
  $\Rightarrow$ use spherical geometry
  2D axisymmetricfull 3D

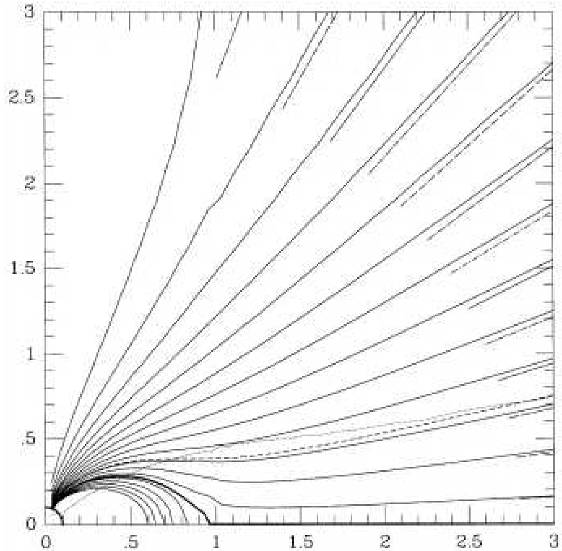

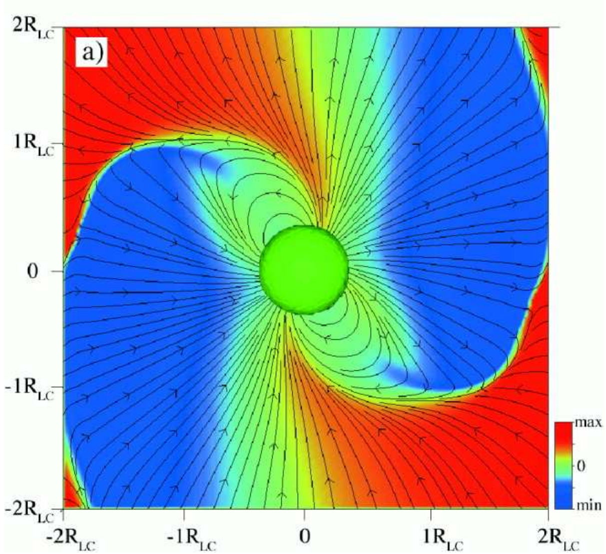

Numerical method

Pseudo-spectral discontinuous Galerkin method

- finite volume formulation in radius.
- high-order interpolation with Legendre polynomials.
- non uniform radial grid (high resolution where needed).
- spectral interpolation in longitude/latitude.
- vector spherical harmonic decomposition.
- 4th order Runge-Kutta time integration.
- Lax-Friedrich flux.
- stabilization by filtering and limiting (avoid overshoot/oscillations).
- exact boundary conditions on the neutron star surface.
- outgoing waves at the outer boundary.

Tested against

- vacuum monopole and Deutsch solution.
- force-free monopole/split monopole.
- GR magnetospheres
- off-centred dipole geometry.

New results on radiative magnetospheres

In an inertial frame

$$\nabla \cdot \mathbf{B} = 0$$

$$\nabla \times \mathbf{E} = -\frac{\partial \mathbf{B}}{\partial t}$$

$$\nabla \cdot \mathbf{E} = \frac{\rho_e}{\varepsilon_0}$$

$$\nabla \times \mathbf{B} = \mu_0 \, \mathbf{j} + \frac{1}{c^2} \frac{\partial \mathbf{E}}{\partial t}.$$

In a corotating coordinate system

$$\frac{\partial \mathbf{B}}{\partial t'} = -\,\mathrm{curl}\,(\mathbf{E} + \mathbf{V}_{\mathrm{rot}} \wedge \mathbf{B})$$

$$\frac{\partial \mathbf{E}}{\partial t'} = \mathrm{curl}\,(c^2 \, \mathbf{B} - \mathbf{V}_{\mathrm{rot}} \wedge \mathbf{E}) - \frac{\mathbf{j}}{\varepsilon_0} + \mathbf{V}_{\mathrm{rot}} \, \mathrm{div}\mathbf{E}.$$

Force-free current

$$\mathbf{j} = \rho_e \frac{\mathbf{E} \wedge \mathbf{B}}{B^2} + \frac{\mathbf{B} \cdot \nabla \times \mathbf{B}/\mu_0 - \varepsilon_0 \, \mathbf{E} \cdot \nabla \times \mathbf{E}}{B^2} \, \mathbf{B}.$$

Radiative current

$$\mathbf{j} = \rho_e \frac{\mathbf{E} \wedge \mathbf{B}}{E_0^2/c^2 + B^2} + (|\rho_e| + 2\,\kappa\, n_0\, e) \frac{E_0 \, \mathbf{E}/c^2 + B_0 \, \mathbf{B}}{E_0^2/c^2 + B^2}$$

Aligned radiative magnetospheres: field lines

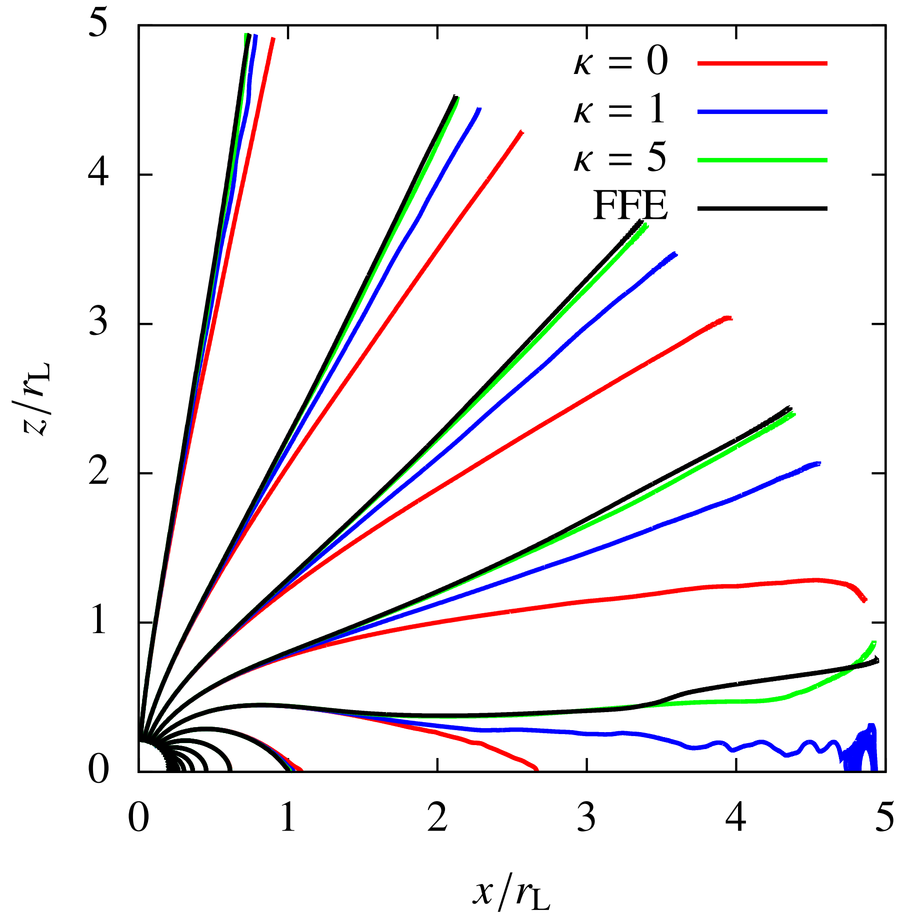

Figure 1: Magnetic field lines for the force-free magnetosphere in black solid lines, and radiative magnetosphere with $\kappa \in \{0, 1, 5\}$ in respectively red, blue and green solid lines as shown in the legend.

Aligned radiative magnetospheres: luminosity

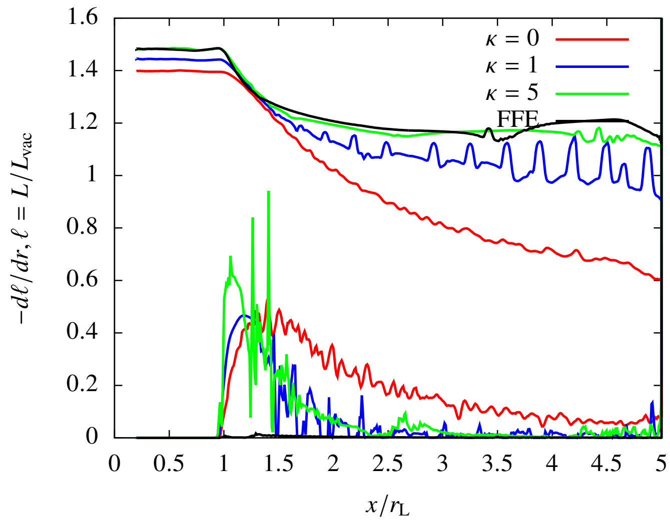

Figure 2: Radial decrease of the Poynting flux. The associated work is shown in the lower curves.

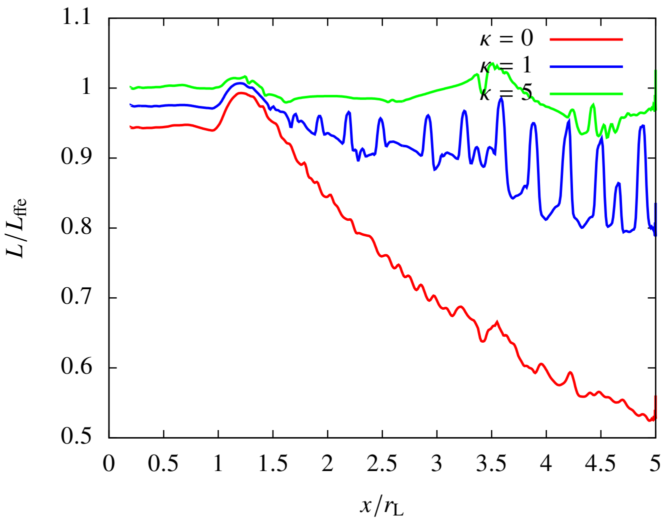

Figure 3: Relative Poynting flux normalized to the FFE spindown.

Aligned radiative magnetospheres: dissipation

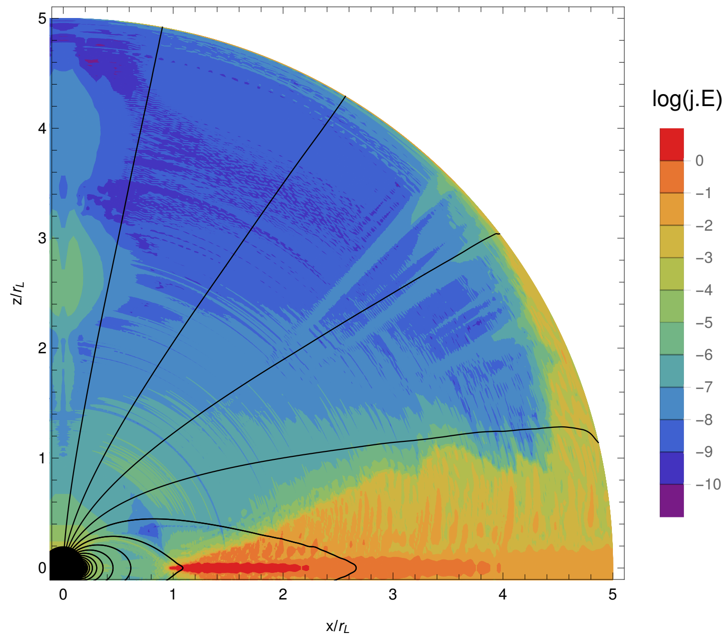

Figure 4: Work done on the plasma for $\kappa = 0$ as given by $\text{æ} \cdot E$.

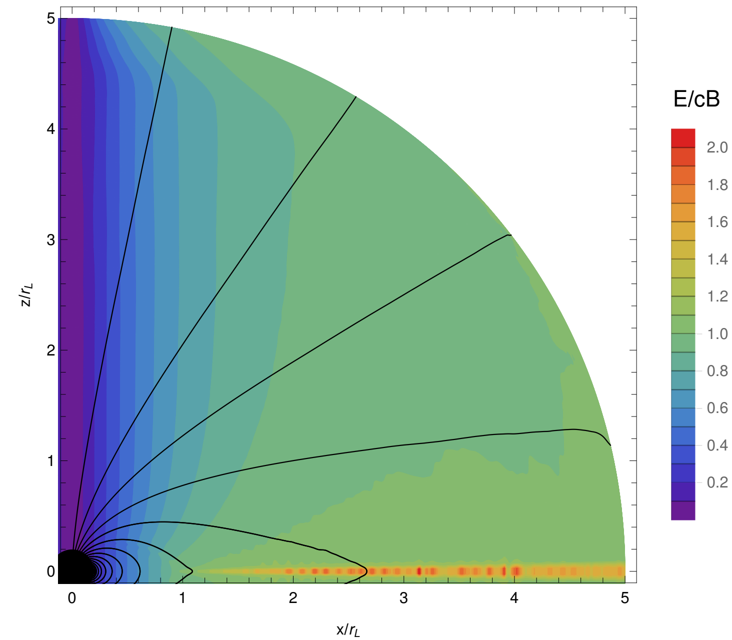

Figure 5: Electric to magnetic field strength ratio E/cB for pair multiplicity $\kappa = 0$.

Orthogonal radiative magnetospheres: field lines

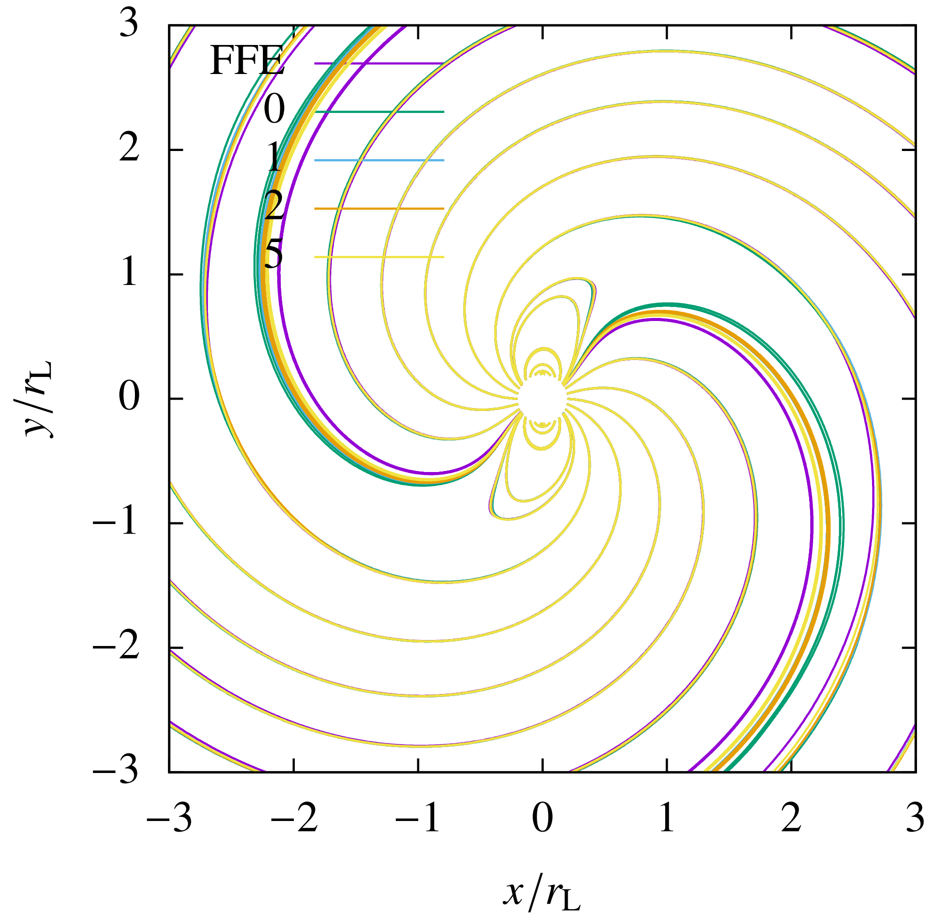

Figure 6: Magnetic field lines for an orthogonal force-free and several radiative magnetospheres.

Orthogonal radiative magnetospheres: dissipation region

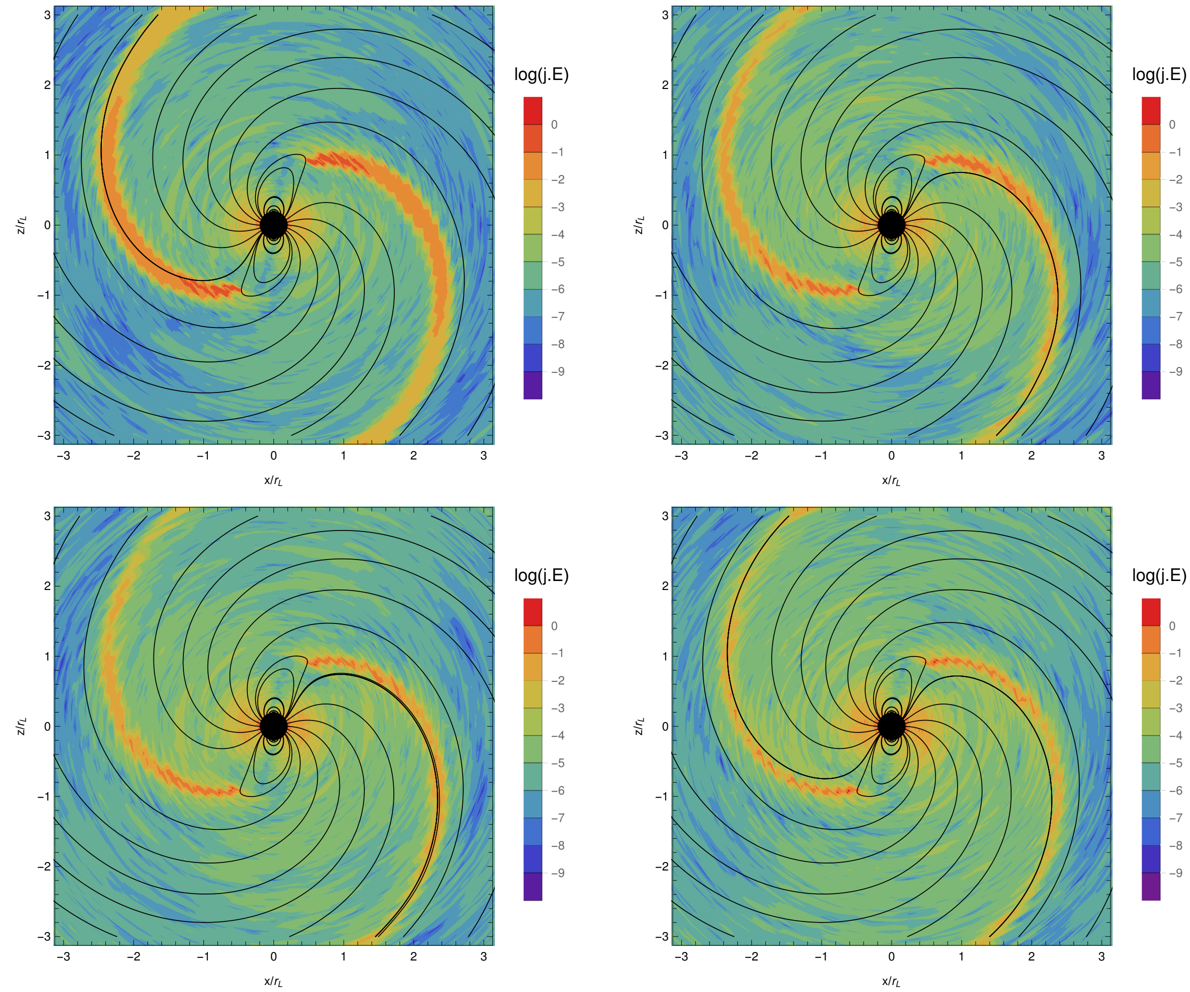

Figure 7: Dissipation in the equatorial plane of an orthogonal rotator for $\kappa = \{0, 1, 2, 5\}$ (from left to right, top to bottom).

Oblique radiative magnetospheres: radial dependence of luminosity

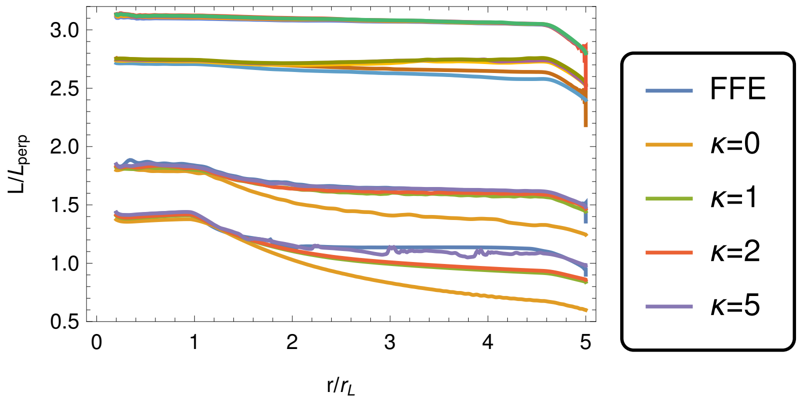

Figure 8: The radial dependence of the Poynting flux of an orthogonal rotator in force-free and radiative regimes.

Oblique radiative magnetospheres: luminosity vs κ and χ

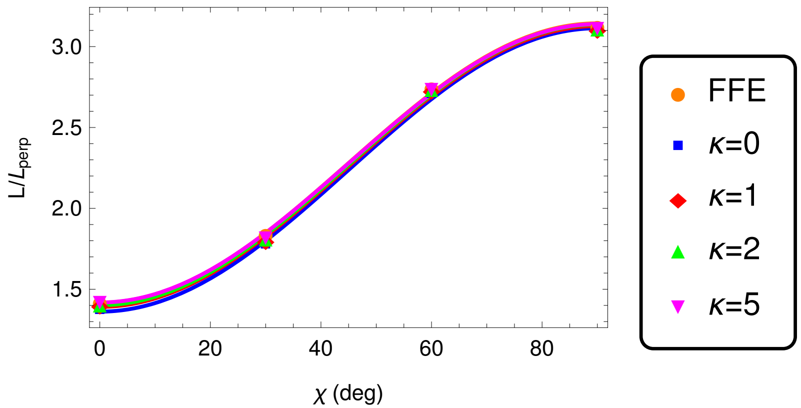

Figure 9: The Poynting flux crossing the light-cylinder for oblique rotators in force-free and radiative regimes.

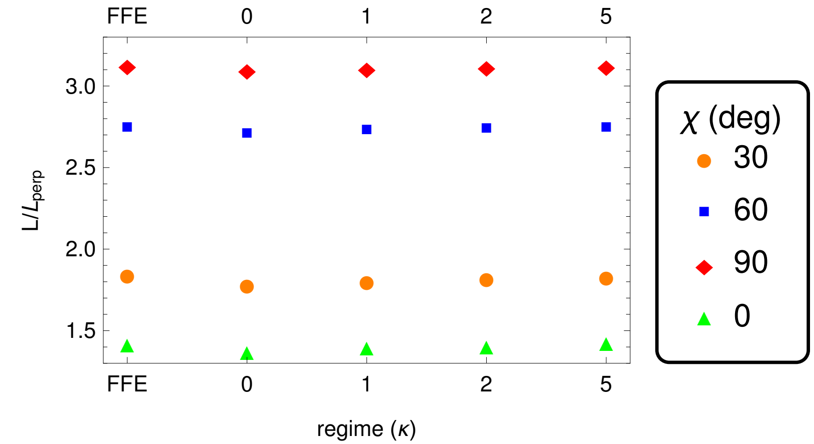

Figure 10: The Poynting flux crossing the light-cylinder for oblique rotators in force-free and radiative regimes.

The problem

- Basic neutron star parameters
  - ✦ magnetic field strength: $B = 10^5 - 10^8$ T.
  - ✦ rotation period: $P = 1\ ms - 10\ s$.
  - ✦ electric field strength: $E = \Omega\, B\, R = 10^{13}$ V/m.
- Two important frequencies
  - ✦ neutron star rotation frequency $\Omega = 2\,\pi / P = 1 - 10^3$ rad/s.
  - ✦ electromagnetic wave frequency $\omega = \frac{e\,B}{m_e} = 10^{16} - 10^{19}$ rad/s.
- The problem with fully kinetic simulations, the strength parameter

$$a = \frac{\omega}{\Omega} = \frac{e\,B}{m_e\,\Omega} = 2{,}8 \cdot 10^{18} \left(\frac{P}{1\ \mathrm{s}}\right) \left(\frac{B}{10^8\ \mathrm{T}}\right) \gg 1 .$$

⇒ impossible to follow individual particle on a timescale P.

⇒ use an analytical pusher not explicitly resolving for the gyration frequency.

Our numerical scheme

Solve analytically the equation in uniform electromagnetic field in the frame where **E** and **B** are parallel (along z) with the electromagnetic field tensor F^{ik}

$$\frac{du^i}{d\tau} = \frac{q}{m} F^{ik} u_k$$

$$F^{ik} = \begin{pmatrix} 0 & 0 & 0 & -E_z/c \\ 0 & 0 & -B_z & 0 \\ 0 & B_z & 0 & 0 \\ E_z/c & 0 & 0 & 0 \end{pmatrix}.$$

Trajectories depend solely on two relativistic electromagnetic invariants

- $\mathcal{I}_1 = E^2 - c^2 B^2$.
- $\mathcal{I}_2 = \mathbf{E} \cdot \mathbf{B}$.

Overview of the algorithm

1. If $\mathcal{I}_2 = \mathbf{E} \cdot \mathbf{B} = 0$ meaning **E** and **B** perpendicular
   - if $\mathcal{I}_1 \neq 0$, frame where either **E** or **B** vanishes exists, depending on the sign of $\mathcal{I}_1$

   $\Rightarrow$ switch to this new frame K' and solve analytically the equation of motion.

   - If $\mathcal{I}_1 = 0$, solve the motion separately as no physical frame K' exist with speed strictly less than c where **E** and **B** are parallel

   $\Rightarrow$ called a null or light like field.

2. If $\mathcal{I}_2 \neq 0$ a frame K' where **E** and **B** are parallel always exists

   $\Rightarrow$ switch to the new frame K' by a Lorentz boost

   $\Rightarrow$ apply an Euler rotation to bring the new z axis along common **E**/**B** direction.

   $\Rightarrow$ solve the particle motion in K'

   $\Rightarrow$ Lorentz boost back to K

Solution to the relativistic equation of motion

For **E** and **B** parallel

$$c\,(t-t_0) = \frac{\gamma_0\,c}{\omega_E}\,\left[\mathrm{sh}(\omega_E\,\tau) + \beta_0^z\,(\mathrm{ch}(\omega_E\,\tau)-1)\right]$$

$$x-x_0 = \frac{\gamma_0\,c}{\omega_B}\,\left[\beta_0^x\,\sin(\omega_B\,\tau) - \beta_0^y\,(\cos(\omega_B\,\tau)-1)\right]$$

$$y-y_0 = \frac{\gamma_0\,c}{\omega_B}\,\left[\beta_0^x\,(\cos(\omega_B\,\tau)-1) + \beta_0^y\,\sin(\omega_B\,\tau)\right]$$

$$z-z_0 = \frac{\gamma_0\,c}{\omega_E}\,\left[(\mathrm{ch}(\omega_E\,\tau)-1) + \beta_0^z\,\mathrm{sh}(\omega_E\,\tau)\right]$$

For null or light like fields

$$c\,(t-t_0) = \gamma_0\,c[\tau + (1-\beta_0^x)\,\frac{\omega_B^2\,\tau^3}{6} + \beta_0^y\,\frac{\omega_B\,\tau^2}{2}]$$

$$x-x_0 = \gamma_0\,c\,[\beta_0^x\,\tau + (1-\beta_0^x)\,\frac{\omega_B^2\,\tau^3}{6} + \beta_0^y\,\frac{\omega_B\,\tau^2}{2}]$$

$$y-y_0 = \gamma_0\,c\,[\beta_0^y\,\tau + (1-\beta_0^x)\,\frac{\omega_B\,\tau^2}{2}]$$

$$z-z_0 = \gamma_0\,v_0^z\,\tau$$

Cross electric and magnetic fields

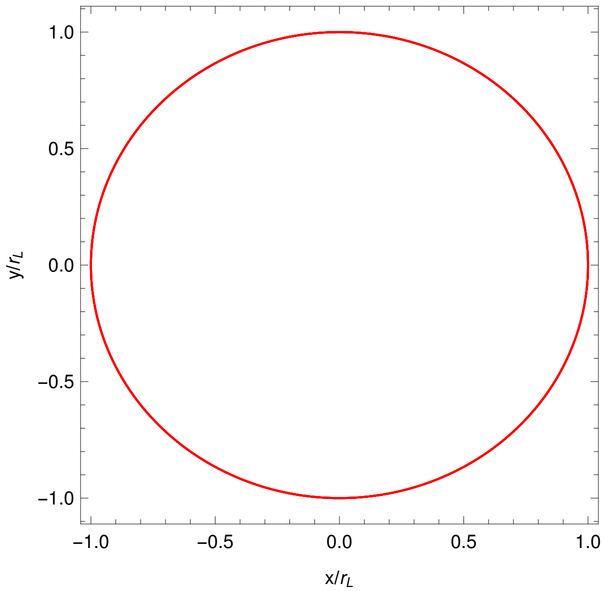

Figure 11: Gyromotion of an electron in the electric drift frame with $\Gamma_E = 10^3$ and $\gamma = 10^{10}$. The Larmor radius is $R_L = 10^{10}$.

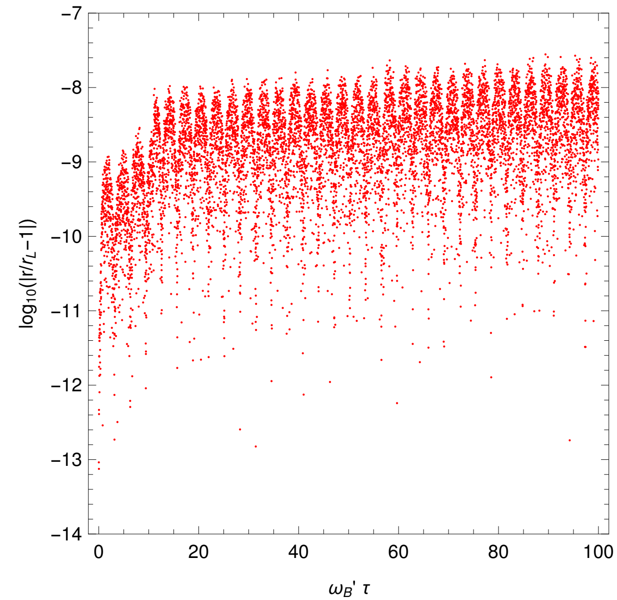

Figure 12: Relative error in the Larmor radius.

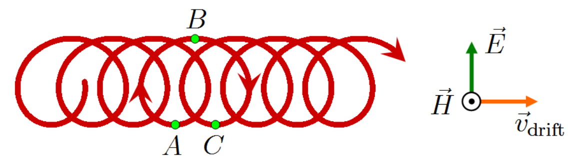

Central electric force

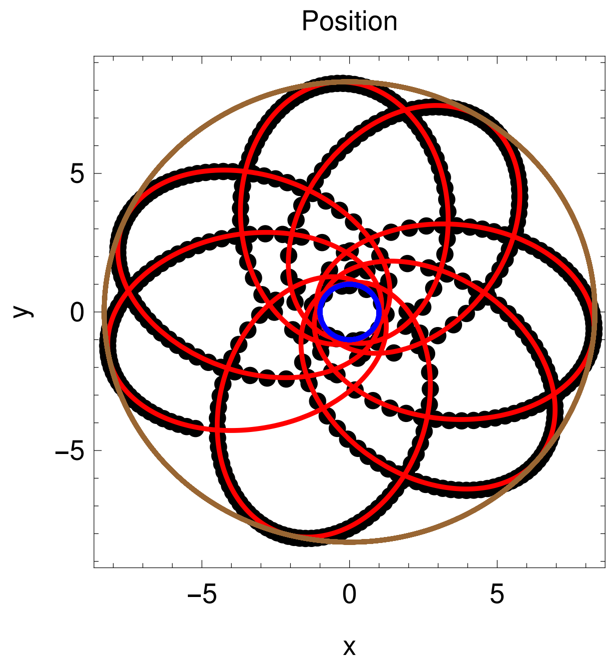

Figure 13: Motion of an electron in the electric field of a fixed proton, black points. Exact analytical solution shown in red.

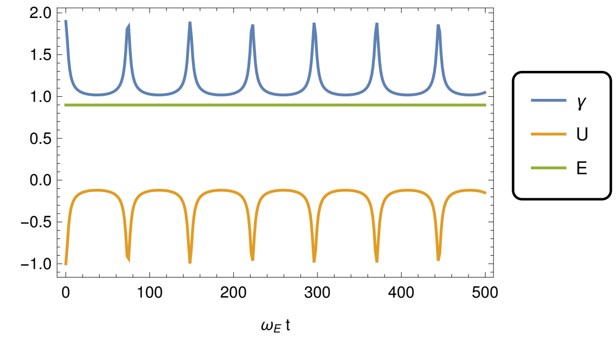

Figure 14: Total energy E, relativistic kinetic energy $\gamma\, m\, c^2$ and electrostatic potential energy U.

Linearly polarized plane wave

Analytical solution given with respect to the wave phase $\xi = \omega\, t - k\, x$ for a particle at rest at initial time $t = 0$.

$$u^x = \frac{a^2}{2}\, c\, (\cos\xi - 1)^2$$
$$u^y = -a\, c\, (\cos\xi - 1)$$
$$u^0 = c + u^x .$$

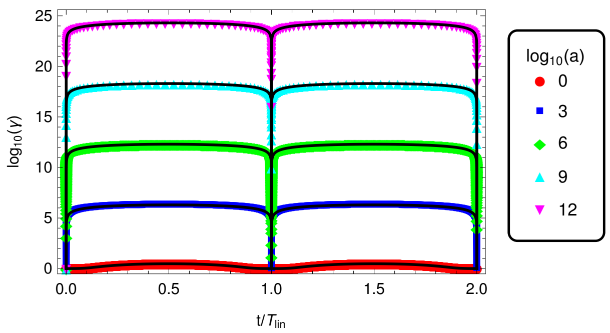

Figure 15: Lorentz factor of an electron for $a = 10^i$ with $i \in \{0, 3, 6, 9, 12, 15\}$.

- Maximum Lorentz factor $\gamma_{\max} = 1 + 2\, a^2$.
- Perfectly period motion with particle returning to rest after a period $P = 2\,\pi\,(1 + 3\, a^2/4)$.
- Ultrarelativistic particles if $a \gg 1$.
- Nonrelativistic particles if $a \ll 1$.

Current state of the art already faces severe flaws at $a \gtrsim 100$ which is unacceptable for neutron stars.

Circularly polarized plane wave

Another analytical solution

$$u^x = a^2\, c\,(1 - \cos\xi) = a\, u^y$$
$$u^y = a\, c\,(1 - \cos\xi)$$
$$u^z = -a\, c\, \sin\xi$$
$$u^0 = c + u^x\,.$$

- Maximum Lorentz factor $\gamma_{\max} = 1 + 2\,a^2$.
- Perfectly period motion with particle returning to rest after a period $P = 2\,\pi\,(1 + a^2)$.

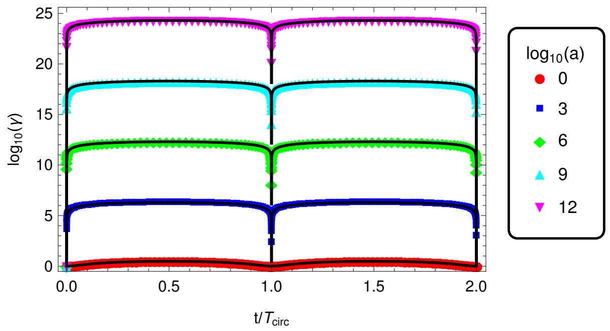

Figure 16: Lorentz factor of an electron for $a = 10^i$ with $i \in \{0, 3, 6, 9, 12, 15\}$.

Particle acceleration in neutron stars: PRELIMINARY RESULTS

Particle distribution functions for several inclinations $\chi = 30°, 60°, 90°, 120°$.

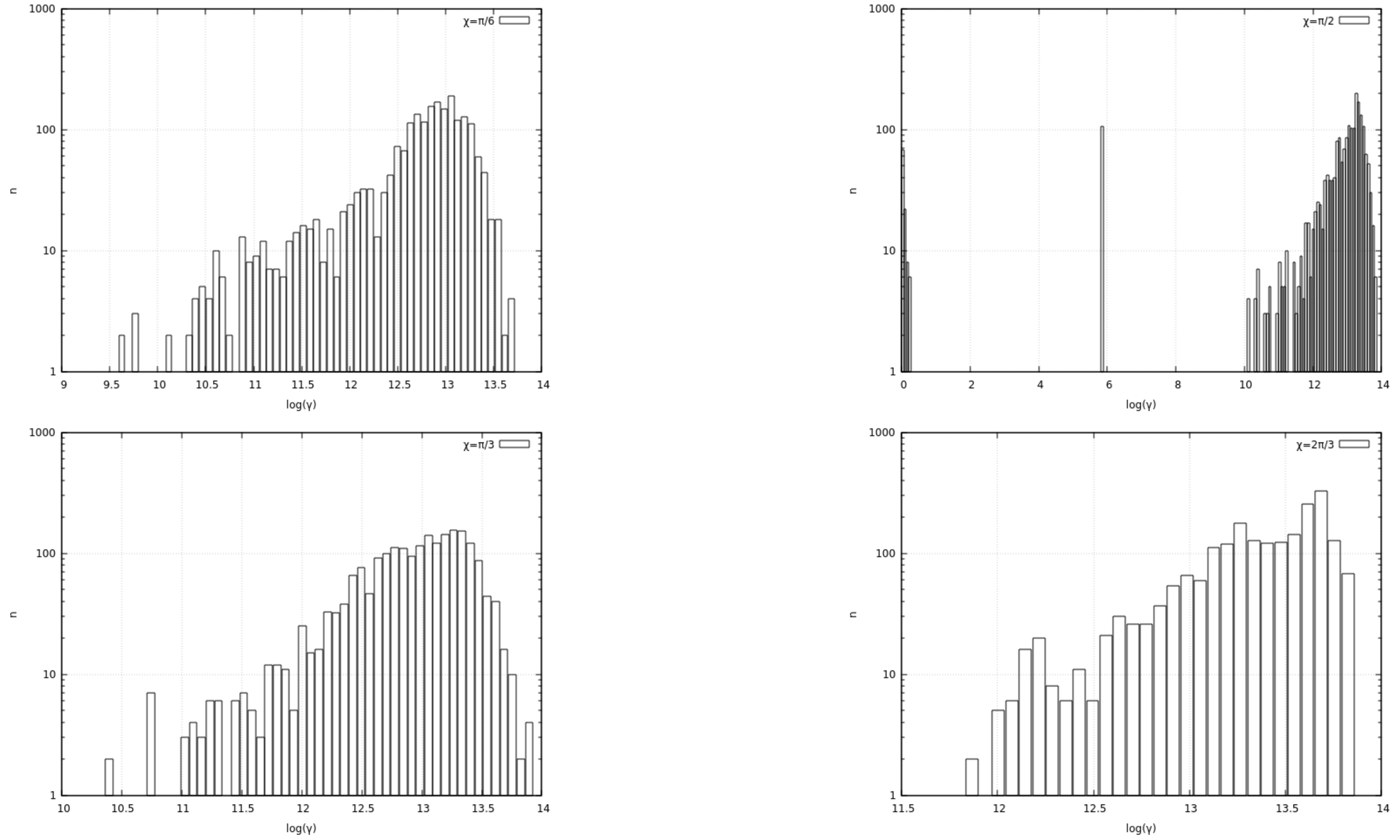

- Maximum Lorentz factor up to $\gamma \approx 10^{13}$
- too high because radiation reaction sets in and slows down the particles probably to $\gamma \approx 10^9$ (to be confirmed by numerical simulations)

Conclusions & Perspectives

- new scheme for particle trajectory integration in any electromagnetic field configuration.
- trajectory is given by an explicit close analytical form.
- for spatially and time dependent fields, numerical errors arise from constant field approximation.
- less stringent condition on the time step.
- approaches well suited for neutron star environment.

- look for analytical solutions in fields that are linear in space and time.
- not clear if such analytical solutions are tractable.
- add radiation reaction at such high Lorentz factors.